Available online at www.sciencedirect.com

ScienceDirect

Procedia Environmental Sciences 31 (2016) 3 – 11

Procedia Environmental Sciences

The Tenth International Conference on Waste Management and Technology (ICWMT)

Adsorption of methylene blue on organosolv lignin from rice straw

Shengli Zhang*, Zhikai Wang, Yulei Zhang, Hongyu Pan, Lichun Tao

Faculty of Geosciences and Environmental Engineering, Southwest Jiaotong University, 610031 Chengdu, Sichuan, China

Abstract

Organosolv lignin (OL) is a relatively pure, unaltered and high-quality lignin, bearing high phenolic and aliphatic hydroxyl contents, which makes it a promising adsorbent in wastewater treatment. In this paper, as a byproduct of delignification of steam-exploded rice straw with the mixed solvents, OL was extracted. The characterization using FTIR, light microscopy and SEM showed that the obtained OL has the typical functional groups of gramineous lignin and a honeycomb-like structure. Batch adsorption studies were carried out for the adsorption of methylene blue (MB) onto the OL. The influences of experimental parameters such as pH, initial dye concentration and contact time were investigated. Results showed that the adsorption of MB on OL was strongly pH-dependent and gave good results in a wide range of pH values (about 5.0～9.0). Compared with pseudo-first-order kinetic model (R^2= 0.935), pseudo-second-order kinetic model (R^2= 0.984) provides a better fit to the adsorption kinetic data. Furthermore, the calculated equilibrium adsorption capacity q_e is 20.38 mg/g which is very similar to the actual amount of adsorption equilibrium (20.62 mg/g). Regarding the adsorption isotherms, Langmuir equation (R^2= 0.999) was more suitable than Freundlich equation (R^2= 0.920). The monolayer capacity of organosolv lignin at 20℃ was 40.02 mg/g, which is comparable with some other lignocelluloses adsorbents reported before.

Peer-review under responsibility of Tsinghua University/ Basel Convention Regional Centre for Asia and the Pacific

Keywords: organosolv lignin, adsorption, methylene blue, adsorption kinetics, adsorption isotherms

1. Introduction

Synthetic dyes are extensively used for textile dyeing, paper printing, color photography and as additives in petroleum products. During the dyeing process, 10-15% of dye is discharged in the effluent, which not only increases the overall loading of chemical oxygen demand to the receiving water but also creates an aesthetic nuisance to the environment even when the concentration is as low as 1ppm [1]. In order to remove dye from industrial effluents, many methods have been tested, such as biological processes, adsorption, coagulation, chemical

Corresponding author. Tel.: +86 028 66367584.
E-mail address: zhang222@home.swjtu.edu.cn

Peer-review under responsibility of Tsinghua University/ Basel Convention Regional Centre for Asia and the Pacific
doi:10.1016/j.proenv.2016.02.001

oxidation processes and photocatalytic degradation [2,3]. Among all of these methods, adsorption has been preferred due to its design simplicity, cheapness, low matrix effects and the possibility to use many classes of materials as adsorbents [4].

Nowadays, byproducts of industrial or agricultural production, such as lignin, sawdust, pine bark, coconut husk, tealeaf and rice hull, are sorts of the low-cost adsorbents [5-7]. Especially, lignin is an important constituent of renewable biomass, which is exceeded in natural abundance only by cellulose. Every year more than 70 million tons of lignin is generated from wastes coming from the pulp and paper and fuel production industries [8], but less than 10% of it is utilized, predominantly as a fuel. Huge amount of lignin is discharged, which is not only a waste of resource but also causes a serious environmental problem. Furthermore, lignin is an aromatic, three-dimensional polymer, containing several important functional groups (ether linkages, aliphatic and aromatic hydroxyl groups) which can be responsible for the adsorptive capacity. So far, lignin as a good adsorbent has been used for the removal of heavy metal ions [9-12], dye [2,3] and organic pollutants [13-14]. However, published studies mainly focus on kraft lignin and hydrolysis lignin, and few ones have been carried out on organosolv lignin (OL). OL is considered as an environmentally friendly and cheap industrial byproduct due to its internal characters such as being quite similar to natural lignin and containing no sulfur [15].

In the present study, as a byproduct of delignification of steam-exploded rice straw with the mixed solvents, OL was prepared in our laboratory. The potential of OL to remove methylene blue (MB) from aqueous media was evaluated as a function of pH, initial dye concentration and contact time. The adsorption process was analyzed according to kinetics and adsorption equilibrium data, and the possible adsorption mechanism of MB molecules on OL was discovered.

2. Materials and methods

1.1. Preparation of organosolv lignin

Air-dried rice straw was collected in suburb of Deyang City of Sichuan Province and pretreated with steam explosion. The steam-exploded rice straw was extracted with water and ethanol sequentially, and then completely dried in an oven under 105±2℃. The delignification of completely dried steam-exploded rice straw was carried by using mixed solvent system consisting of water, N,N-dimethylformamide and aniline acting as catalyst (in ratio of 100/50/5, V/V/V). The solution (black liquor) containing lignin was concentrated by vacuum distillation, at the same time, the mixed solvent was recycled. Complete precipitation of OL was observed during the process of dilution when the ratio of water to concentrated black liquor was up to 5. The precipitated OL was washed using hot distilled water until the supernatant became nearly colorless. Finally, the washed sample was dried in the oven at 70℃ and ground in the mill.

1.2. Characterization of organosolv lignin

To investigate the functional groups of OL, fourier transform infrared spectroscopy (FT-IR) was obtained on an FT-IR spectrophotometer Nicolet 5700 (Thermo, USA) using a KBr disc containing 1% finely ground sample. Sixty-four scans were taken for each sample from 4000 to 400 cm^{-1} at a resolution of 4 cm^{-1} due to the lignin related intensities.

The morphology of OL was respectively observed with an optical microscope and a Quanta 200 SEM (FEI Com, Holland) which was operated in secondary electron mode at an accelerating voltage of 20 kV. Prior to Scanning electron microscopy (SEM) imaging of the sample, the solid particles were coated with a gold film to improve their conductivity and the quality of the SEM images.

1.3. Batch adsorption experiments

A stock solution of MB (200 mg/L) was prepared by dissolving an appropriate quantity of MB in distilled water, and then the stock solution was diluted to the desired concentrations. Batch experiments were conducted in 100 mL Erlenmeyer flask by adding 0.1g of OL to 50mL of MB aqueous solutions（10-200 mg/L）. The mixtures were

agitated for a suitable period of time (10 min to 24 h) at 20°C. The pH of MB solutions, which ranged from 3.0 to 9.0, was adjusted by 1 mol/L NaOH and 1 mol/L HCl. At the end of each adsorption batch runs, the adsorbent was separated from the aqueous solution by centrifugation at 4000 rpm for 10 min. The final amounts of MB which remained in the solution were determined at the maximum wavelength 664 nm using a 722S spectrophotometer. The amount of adsorption was calculated according to equation (1):

$$q = \frac{(C_0 - C_f)V}{m} \tag{1}$$

Where q is the amount of MB taken up by OL, C_0 and C_f are the initial and final concentrations of MB in solution, m is adsorbent mass and V is the volume of MB solution. All adsorption experiments were conducted in triplicate and the results were averaged.

1.4. Kinetic and equilibrium models

The kinetics of adsorption was evaluated by using pseudo-first-order kinetic model (Eq. (2)) and pseudo-second-order kinetic model (Eq. (3)) , respectively.

$$q = q_e(1 - \exp(-k_1 t)) \tag{2}$$

$$q = \frac{k_2 q_e^{\,2} t}{1 + k_2 q_e t} \tag{3}$$

where k_1 is the rate constant for the pseudo-first-order kinetic equation, k_2 is the rate constant for the pseudo-second-order kinetic equation q_e and q are the amounts of MB adsorbed at equilibrium and at time t, respectively.

The equilibrium of adsorption was evaluated by using Langmuir isotherm model (Eq. (4)) and Freundlich isotherm model (Eq. (5)), respectively.

$$\frac{C_e}{q_e} = \frac{1}{K_L q_{\max}} + \frac{C_e}{q_{\max}} \tag{4}$$

$$\ln q_e = \ln K_F + \frac{1}{n} \ln C_e \tag{5}$$

where K_L is the Langmuir equilibrium constant, q_{max} is the maximum monolayer uptake capacity of the adsorbent and C_e is the dye concentration at the equilibrium; K_F is the Freundlich equilibrium constant which indicates the multilayer adsorption capacity of the adsorbent, $1/n$ gives a measure of the intensity of adsorption.

3. Results and discussion

3.1. *Structure and morphology of organosolv lignin*

The spectrum of a lignin sample can give an overall view of its chemical structure [16]. Fig. 1 shows the FT-IR spectrum of OL obtained. The strong absorption at 3400 cm^{-1} is attributed to OH stretching, while bands at 2920, 2850 and 1445 represent C–H anti-symmetric and symmetric stretching of CH_2 and CH_3 groups [17]. The characteristic three peaks at 1600, 1500 and 1425 cm^{-1} are assigned to aromatic skeleton vibrations in herbaceous lignin, which were reported in previous literature [18,19]. The cleavage of the β–O–4 and α–O–4 linkages, which leaves a lot of non-etherified phenolic OH groups in lignin, is visible at 1376 cm^{-1}. Bands between 694 and 1317 cm^{-1} are indicative of the presence of guaiacyl (G), hydroxy-phenyl (H) and syringyl (S) units [20,21], in which absorption at 1317 cm^{-1} is related to S unit plus G unit condensed and that at 1160 cm^{-1} H unit. The wide peak at 1258 cm^{-1} is attributed to C–O stretching of the aromatic skeletons in S and G units. The bands at 1100, 1060 and 1035 cm^{-1} arise from C–H in-plan deformation for S type and G type. In addition, the absorption bands at low wave numbers are related to the position of substituting group on phenyl ring.

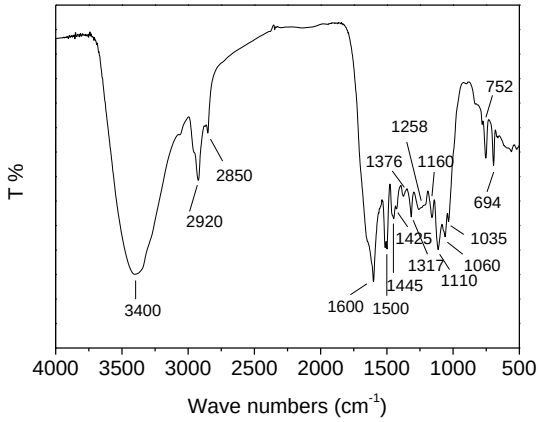

Fig. 1. FT-IR spectrum of OL

The optical micrograph (Fig. 2) was obtained with an XSZ-3G microscope with magnification 100×. It can be seen that OL particles are globule and have a strong tendency to agglomerate. Xu et al. [22] also reported that the dissolved lignin coagulates into lignin globules in the ethanol-based organosolv pulping. Although the exact structure of OL has not been elucidated, it is generally accepted that OL not only contains hydrophobic groups, such as aromatic and aliphatic groups, but also contains many hydrophilic groups, such as carbonyl, phenolic and aliphatic hydroxyl groups [23,24]. Therefore, OL particles can produce strong adsorption force by hydrogen bond interaction and cause aggregation. Compared with OL, the hydrogen bond interaction in lignosulfonate is different, which is due to sulfonic, carboxyl and phenolic hydroxyl groups [25]. With the consideration of the limitation of transmission optical microscopy, SEM was used to further investigate the surface morphology of OL particles. As seen in Fig. 3, individual particle of OL has a honeycomb-like structure, which is propitious to adsorbate permeating the interior of OL. The hydrophobic core is loose and contains many weakly ionized groups such as carboxyl and phenolic hydroxyl groups. Thus, the adsorption of adsorbate on the exterior and interior of OL can simultaneously be promoted.

Fig. 2. Optical microscopic image of OL

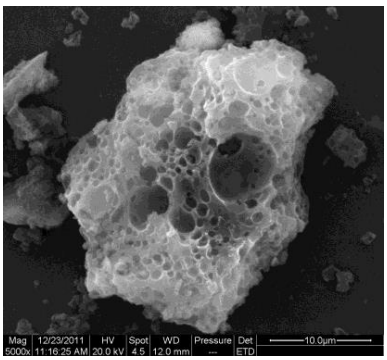

Fig. 3. SEM image of OL

3.2. *Effect pH on adsorption of MB on organosolv lignin*

Generally, medium acidity is one of the most important factors in adsorption studies [26,27]. Different species may present divergent ranges of suitable pH depending on which adsorbent is used. In the present study, the adsorption of MB on OL was studied within the pH range of 3 ~ 9. The effects of pH on the adsorption amount and

the MB removal are shown in Fig. 4. It is obvious that the adsorption of MB on OL is highly pH-dependent and can give good results in a wide range of pH values. The adsorption amount of MB dramatically increased from 14.62 mg/g to 18.85 mg/g with increasing pH values from 3.0 to 4.0. Thereafter, the increment decreased and tended to stabilize over a wide range of pH values (about 5.0～9.0). Such adsorption trend could be due to the competition between cationic dye and proton for the binding sites on OL surface. The pH-dependence of adsorption suggests that adsorption process follows the ion-exchange mechanism [28]. OL has high phenolic and aliphatic hydroxyl contents, which is easy to be protonated or deprotonated at different pH values. The dissolved MB dye is positively charged in water solution, whose adsorption takes place when the adsorbent presents negative surface charge. At low pH (pH < 3), OL presented a positive surface charge since the surface functional groups were protonated, which caused strong electrostatic repulsion between OL and MB molecules, hindering the cationic dye-binding process. When the pH of solution increased from 3.0 to 5.0, OL gradually appeared a negative surface charge owing to deprotonation of its surface functional groups, which was favorable for the electrostatic attraction of MB molecules in solution and finished the ion-exchange process.

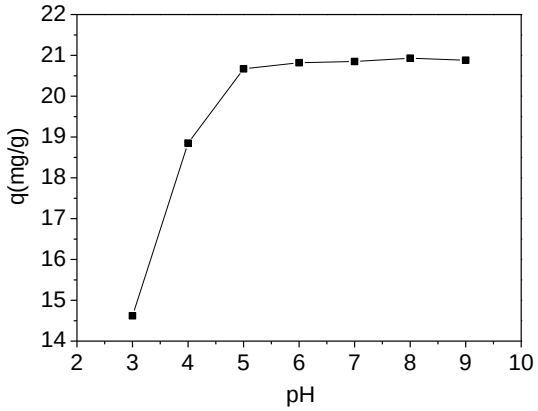

Fig. 4. Effect of pH on the adsorption of MB on OL

3.3. *Effect of contact time and adsorption kinetics*

In order to determine the time required for reaching the adsorption equilibrium, MB solutions (50 mg/L) were absorbed by OL for different time. The effect of contact time on the adsorption amount of MB on OL was displayed in Fig. 5. It can be observed that the adsorption amount increases sharply in the first 10 minutes, then increases tardily and tends to stabilize after 120 minutes. Adsorption kinetic studies are important because they can provide valuable information on the mechanism of adsorption process [29]. According to the adsorption data obtained from the experiment, pseudo-first-order kinetic model and pseudo-second-order kinetic model were employed to elucidate the potential rate-controlling steps and to predict the adsorption kinetics. The constants of different kinetic models were depicted in Table 1. The correlation coefficient (R^2) of pseudo-first-order kinetic equation is 0.935, and the calculated equilibrium adsorption capacity q_e is 19.47 mg/g. Comparatively speaking, a perfect fitting was obtained by pseudo-second-order kinetic equation with a higher correlation coefficient (R^2= 0.984). Furthermore, the calculated equilibrium adsorption capacity q_e is 20.38 mg/g which is very similar to the experimental amounts 20.62 mg/g of adsorption equilibrium. In the majority studies on kinetic process of dye adsorption on various adsorbents, a similar two-step behavior was reported [30-32]. Generally, the overall rate of adsorption process is controlled by the slowest rate-limiting step. The pseudo-second-order kinetic model is based on the assumption that the rate-limiting step is a chemical adsorption involving valance force through sharing or exchange of electrons between adsorbent and adsorbate [33,34]. Hence, ion-exchange is the rate-controlling step in the present study. The two steps of adsorption process include a fast initial physisorption followed by a much slower gradual chemisorption. The former is attributed to the diffusional process of the cationic dye to the adsorbent surface, and the latter to ion-exchange mechanism.

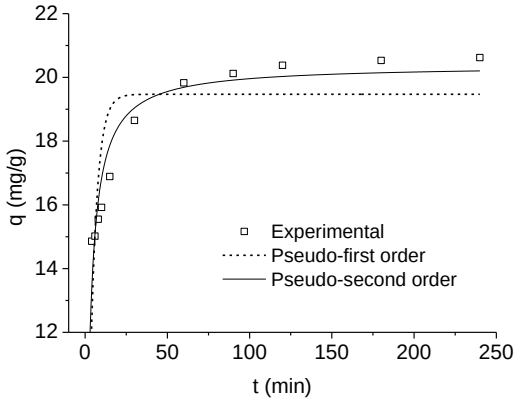

Fig. 5. Adsorption kinetic curve and kinetic models of MB onOL: (a) Pseudo-first-order kinetic model, (b) Pseudo-second-order kinetic model.

Table 1. Comparison of pseudo-first-order kinetics and pseudo-second-order kinetics constants and experimental and calculated q_e values.

$q_{e(exp)}$ (mg/g)	Pseudo-first-order kinetics			Pseudo-second-order kinetics		
	k_1 (min^{-1})	$q_{e(cal)}$ (mg/g)	R^2	k_2 (g/(mg min))	$q_{e(cal)}$ (mg/g)	R^2
20.62	0.258	19.47	0.935	0.023	20.38	0.984

3.4. *Adsorption equilibrium and isotherm models*

The adsorption isotherm plays important role in describing how the adsorbate interacts with the adsorbent and gives an idea adsorption capacity of the adsorbent. In this study, the adsorption equilibrium experiments were performed with the initial MB concentrations varied from 10 to 200 mg/L. When the initial MB concentration was below 100 mg/L, adsorption capacity of OL increased linearly with increasing the initial MB concentrations (see Fig. 6). Then a slow increase was observed and the maximum capacity was reached, approximately 38.5 mg/g. It is important in estimation of practical adsorption capacity and optimization of adsorption systems design to analyze the adsorption equilibrium data using different isotherm models. The Freundlich isotherm assumes non-ideal adsorption on heterogeneous surfaces and multilayer adsorption, whereas Langmuir isotherm is used for the monolayer adsorption on a homogenous surface. The fitting results of adsorption isotherms by Langmuir model and Freundlich model are showed in Fig. 6a and b. Meanwhile, the isotherm parameters for different models are presented in Table 2. The best-fit equilibrium model can be established based on the linear regression correlation coefficients (R^2). Compared with Freundlich equation with the R^2 value of 0.920, Langmuir equation (R^2= 0.999) gives a better fit to the adsorption isotherm of MB on OL. Suteu et al. [3] obtained the similar results when industrial lignin was used to remove reactive dye Brilliant Red HE-3B from aqueous solutions. This might indicate that the adsorption sites on the surface of OL are homogenous and the adsorption of cationic dye MB is the monolayer adsorption. According to the result of Langmuir analysis, the monolayer capacity of OL at the temperature of 20℃ was 40.02 mg/g, which is comparable with most other lignocellulose sorbents mentioned in literatures reported before [35-37].

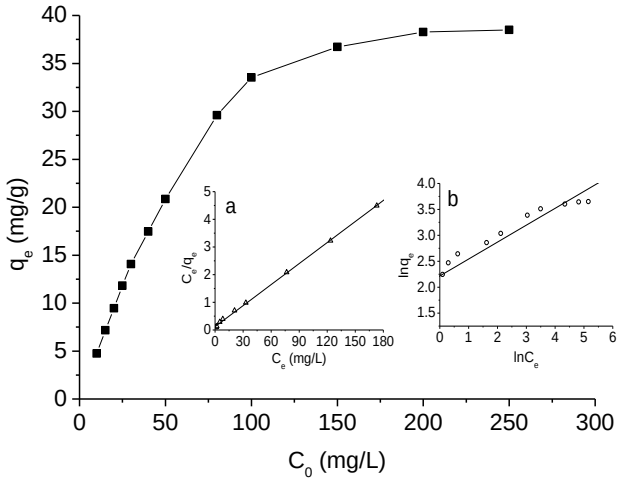

Fig. 6. Adsorption isotherm curves and isotherm models of MB on OL: (a) Langmuir model, (b) Freundlich model.

Table 2. Characteristic parameters obtained by the Freundlich and Langmuir equations

Langmuir constant			Freundlich constant		
K_L (L/mg)	q_{max} (mg/g)	R^2	n_F (g/L)	K_F (mg/g)	R^2
0.2083	40.02	0.999	3.0675	9.1706	0.920

4. Conclusion

OL made using a mixed solvent delignification of SERS comprises of G, H and S units and has a honeycomb-like structure. Because of the hydrogen bond interaction among hydrophilic groups, such as carbonyl, phenolic and aliphatic hydroxyl groups, OL shows a strong tendency to agglomerate in the optical micrograph. The honeycomb-like structure can facilitate the adsorption of adsorbate on the exterior and interior of OL. The adsorption of MB on OL is strongly pH-dependent and can give satisfied results in a wide range of pH values. The adsorption amount increased dramatically from 14.62 mg/g to 18.85 mg/g when pH value increased from 3.0 to 4.0, while the increment decreased after that, and tended to stabilize over a wide range of pH values (about 5.0 ~ 9.0). Compared with pseudo-first-order kinetic model (R^2= 0.935), pseudo-second-order kinetic model provides a better fit to the adsorption kinetic data with a correlation coefficient (R^2= 0.984). Furthermore, the calculated equilibrium adsorption capacity q_e is 20.38 mg/g which is very similar to the experimental amounts 20.62 mg/g of adsorption equilibrium. Therefore, chemisorption is the rate-controlling step in the present study. Regarding the fitting of adsorption isotherms, Langmuir equation (R^2= 0.999) is more suitable than Freundlich equation (R^2=0.920). The monolayer capacity of OL at temperature of 20℃ is 40.02 mg/g, which is comparable with most other lignocelluloses adsorbents reported before.

Acknowledgements

The present work was financially supported by National Natural Science Foundation of China (51303151), Science & Technology Pillar Programof Sichuan Province (2015GZ0230) and the Fundamental Research Funds for the Central Universities (2682014CX011).

References

1. Al-Degs Y, Khraisheh MAM, Allen SJ, hmad MNA. Effect of carbon surface chemistry on the removal of reactive dyes from textile effluent. *Water Res* 2000;34:927-5.
2. da Silva LG, Ruggiero R, Gontijo PM, Pinto RB, Royerb B, Lima EC, Fernandes THM, Calvete T. Adsorption of brilliant red 2BE dye from water solutions by a chemically modified sugarcane bagasse lignin. *Chem Eng J* 2011; 168:620-8.
3. Suteu D, Malutan T, Bilba D. Removal of reactive dye Brilliant Red HE-3B from aqueous solutions by industrial lignin: Equilibrium and kinetics modelling. *Desalination* 2010; 255:84-90.
4. Qadeer R. Adsorption behavior of ruthenium ions on activated charcoal from nirtic acid medium. *Colloids Surf A: Physicochem Eng Aspects* 2007;93:217-23.
5. Guo XY, Zhang SZ, Shan XQ. Adsorption of metal ions on lignin. *J Hazard Mater* 2008; 151:134-42.
6. Lataye DH, Mishra IM, Mall ID. Adsorption of α-picoline onto rice husk ash and granular activated carbon from aqueous solution: equilibrium and thermodynamic study. *Chem Eng J* 2009; 147:139-49.
7. Chen S, Yue Q, Gao B, Xu X. Equilibrium and kinetic adsorption study of the adsorptive removal of Cr(VI) using modified wheat residue. *J Coll Inter Sci* 2010;349:256-64.
8. Satheesh Kumar MN, Mohanty AK, Erickson L, Misra M. Lignin and its applications with polymers. J Biobased Mater Bio 2009; 3: 1-24.
9. Demirbas A. Adsorption of lead and cadmium ions in aqueous solutions onto modified lignin from alkali glycerol delignication. *J Hazard Mater* B 2004;109:221-6.
10. Mohan D, Pittman Jr CU, Steele PH. Single, binary and multicomponent adsorption of copper and cadmium from aqueous solutions on Kraft lignin—a biosorbent. *J Colloid Interf Sci* 2006;297:489-504.
11. Brdar M, Šćiban M, Takači A, Došenović T. Comparison of two and three parameters adsorption isotherm for Cr(VI) onto Kraft lignin. *Chem Eng J* 2012;183:108-11.
12. Lv J, Luo L, Zhang J, Chrstie P, Zhang S. Adsorption of mercury on lignin: Combined surface complexation modeling and X-ray absorption spectroscopy studies. *Environ Pollut* 2012;162:255-61.
13. Zhang JP, Lin XY, Luo XG, Zhang C, Zhu H. A modified lignin adsorbent for the removal of 2,4,6-trinitrotoluene. *Chem Eng J* 2011;168:1055-63.
14. Saad R, Radovic-Hrapovic Z, Ahvazi B, Thiboutot S, Ampleman G, Hawari J. Sorption of 2,4-dinitroanisole (DNAN) on lignin. *J Environ Sci* 2012;24:808-13.
15. Acemioğlu B, Samil A, Alma MH, Gundogan R. Copper(II) Removal from aqueous solution by organosolv lignin and its recovery. *J Appl Polym Sci* 2003;89:1537-41.
16. Gilarranz MA, Rodriguez F, Oliet M, Garcia J, Alonso V. Phenolic OH group estimation by FTIR and UV spectroscopy application to organosolv lignins. *J Wood Chem Technol* 2001;21:387-95.
17. Xiao LP, Shi ZJ, Xu F, Sun RC, Mohanty AK. Structural characterization of lignins isolated from caragana sinica using FT-IR and NMR spectroscopy. *Spectrosc Spect Anal* 2011;31:2369-76.
18. Jahan MS, Chowdhury DAN, Islam MK, Moeiz SMI. Characterization of lignin isolated from some nonwood available in Bangladesh. *Bioresour Technol* 2007;98:465-9.
19. Xu F, Geng ZC, Liu CF, Ren JL, Sun JX, Sun RC. Structural characterization of residual lignins isolated with cyanamide-activated hydrogen peroxide from various organosolvs pre-treated wheat straw. *J Appl Polym Sci* 2008;109:555-64.
20. Cai Y, Li G, Nie J, Lin Y, Nie F, Zhang J, Xu Y. Study of the structure and biosynthetic pathway of lignin in stone cells of pear. *Scientia Horticulturae* 2010;125:374-9.
21. Tejado A, Peña C, Labidi J, Echeverria JM, Mondragon I. Physico-chemical characterization of lignins from different sources for use in phenol-formaldehyde resin synthesis. *Bioresour Technol* 2007;98:1655-63.
22. Xu YJ, Li KC, Zhang MY. Lignin precipitation on the pulp fibers in the ethanol-based organosolv pulping. *Colloids Surf A: Physicochem Eng Aspects* 2007;301:255-63.
23. El Mansouri NE, Salvadó J. Analytical methods for determining functional groups in various technical lignins. *Ind Crop Prod* 2007;26:116-24.
24. EI Hage R, Brosse N, Chrusciel L, Sanchez C, Sannigrahi P, Ragauskas A. Characterization of milled wood lignin and ethanol organosolv lignin from miscanthu. *Polym Degrad Stable* 2009;94:1632-8.
25. Yan MF, Yang DJ, Deng YH, Chen P, Zhou HF, Qiu XQ. Influence of PH on the behavior of lignosulfonate macromolecules in aqueous solution. *Colloids Surf A: Physicochem Eng Aspects* 2010;371:50-8.
26. Lima EC, Royer B, Vaghetti JCP, Brasil JL, Simon NM, dos Santos Jr AA, Pavan FA, Dias SLP, Benvenutti EV, da Silva EA. Adsorption of Cu(II) on Araucaria angustifolia wastes: determination of the optimal conditions by statistic design of experiments. *J Hazard Mater* 2007;140:211-20.
27. Calvete T, Lima EC, Cardoso NF, Dias SCP, Pavan FA. Application of carbon adsorbents prepared from the Brazilian-pine fruit shell for removal of Procion Red MX 3B from aqueous solution-kinetic, equilibrium, and thermodynamic studies. *Chem Eng J* 2009;155:627-36.
28. Yu LJ, Shukla SS, Dorris KL, Shukla A, Margrave JL. Adsorption of chromium from aqueous solutions by maple sawdust. *J Hazard Mater* 2003;100:53-63.
29. Oladoja NA, Akinlabi AK. Congo red biosorption on palm kernel seed coat. *Ind Eng Chem Res* 2009;48:6188-96.
30. Bulut Y, AydIn H. A kinetics and thermodynamics study of methylene blue adsorption on wheat shells. *Desalination* 2006;194:259-67.
31. Ponnusami V, Vikram S, Srivastava SN. Guava (Psidium guajava) leaf powder: novel adsorbent for removal ofmethylene blue fromaqueous solutions. *J Hazard Mater* 2008;152:276-86.
32. Lakshmi UR, Srivastava VC, Mall ID, Lataye DH. Rice husk ash as an effective adsorbent: evaluation of adsorptive characteristics for Indigo Carmine dye. *J Environ Manage* 2009;90:710-20.
33. Mohan D, Singh KP, Singh VP. Trivalent chromium removal from wastewater using low cost activated carbon derived from agricultural waste material and activated carbon fabric cloth. *J Hazard Mater* 2006;135:280-95.
34. Ibrahim K, Mehmet U, Hamdi K, Ali Ç. Adsorption of Cd(II) ions from aqueous solutions using activated carbon prepared from olive stone

by $ZnCl_2$ activation. *Bioresour Technol* 2008;99:492-501.
35. Longhinotti E, Pozza F, Furlan L, Sanchez MNM, Klug M, Laranjeira MCM, Fávere VT. Adsorption of anionic dyes on the biopolymer chitin. *J Braz Chem Soc* 1998;9:435-40.
36. Consolin Filho N, Venancio EC, Barriquello MF, Hechenleitner AAW, Pineda EAG. Methylene blue adsorption onto modified lignin from sugar cane bagasse. *Eclet Quím* 2007;32:63-70.
37. Suteu D, Zaharia C, Malutan T. Removal of Orange 16 reactive dye from aqueous solutions by waste sunflower seed shells. *J Serb Chem Soc* 2011;76:607-24.